Mechanism for microwave degradation of Methylene Blue and Arsenazo(III) dyes using graphene oxide synthesized from date pits

Nasser S. Awwad[a,b,*], A.Y. Alshahrani[c], Ehab. El Sayed Massoud[d,e], A. Bouzidi[f,g], Mai S.A. Hussein[h,i], I.S. Yahia[i,j]

[a]*Chemistry Department, Faculty of Science, King Khalid University, P.O. Box: 9004, Abha 61413, Saudi Arabia,*
email: aawwad@kku.edu.sa (N.S. Awwad)
[b]*Research Centre for Advanced Materials Science (RCAMS), King Khalid University, P.O. Box: 9004, Abha 61413, Saudi Arabia*
[c]*Faculty of Medicine, King Khalid University, P.O. Box: 9004, Abha 61413, Saudi Arabia (A.Y. Alshahrani)*
[d]*Department of Biology, Faculty of Sciences and Arts in Dahran Aljanoub, King Khalid University, Saudi Arabia,*
email: ehabheca@gmail.com (E. El Sayed Massoud)
[e]*Agriculture Research Center, Soil, Water, and Environment Research Institute, Giza, Egypt*
[f]*Research Unit, Physics of Insulating and Semi-insulating Materials, Faculty of Sciences, University of Sfax,*
B.P. 1171, 3000 Sfax, Tunisia (A. Bouzidi)
[g]*Technical and Vocational Training Corporation: Technical College Branch, P.O. Box: 10 Post Code: 61974, Ahad Rufidah,*
Kingdom of Saudi Arabia
[h]*Department of Chemistry, Faculty of Education, Ain Shams University, Roxy 11757, Cairo, Egypt (M.S.A. Hussein)*
[i]*Nanoscience Laboratory for Environmental and Bio-medical Applications (NLEBA), Semiconductor Lab., and Department of Physics,*
Faculty of Education, Ain Shams University, Roxy 11757, Cairo, Egypt (I.S. Yahia)
[j]*Advanced Functional Materials and Optoelectronic Laboratory, Department of Physics, Faculty of Science,*
King Khalid University, P.O. Box: 9004, Abha, Saudi Arabia

ABSTRACT

Many methods, such as biodegradation, ultra-filtration, photocatalytic degradation, oxidation, and adsorption, have been used in wastewater treatment. Adsorption is a conventional wastewater treatment technique that is comparatively cheap and efficient. The aim of this work is to determine the effectiveness of degradation of a novel technique of microwave radiation against methylene blue (MB) dye and arsenazo III dye using graphene oxide (GO) synthesized from Saudi date pits. The conversion of date pits to GO takes place first through two steps, the conversion of date pits to active carbon and then to GO. The characteristics of the samples were scanning electron microscopy, Fourier transform/Raman, Surface, Fourier transformation infrared spectroscopy, X-ray diffraction, and ultraviolet-visible absorption. MB and Arsenazo III dyes degradation was monitored as a function of irradiation time by measuring maximum absorbance. Measurements were taken for chemical oxygen demand (COD) and biological oxygen demand (BOD). Kinetic models was studied via pseudo-first-order, pseudo-second-order, and elovich. It was found that both chemical and surface adsorption mechanisms are participating in the studied systems.

Keywords: Graphene oxide; Cationic dyes; Wastewater treatment; Adsorption; Degradation; COD; BOD

* Corresponding author.

1. Introduction

Textile plant effluents contain portions of coloring used in industries like textiles, paper, plastics, tannery, and paints. The amount of dyes produced is estimated to be important sources of water pollution, some dyes, and their products for degradation may be carcinogens and toxic. Before disposal, therefore, the dyes must be treated. Organic pollution occurs when huge amounts of organic compounds affect household sewage, urban run-off, industrial effluents, and wastewater from agriculture. The dissolved oxygen in the receiving water can be consumed at a higher rate than it can be replenished during the organic pollutant decomposition process, causing depletion of oxygen and having severe effects on the biota stream. Due to acute toxicity and the carcinogenic nature of the pollutants, water pollution due to organic contaminants is a significant issue. Water pollution is water bodies such as lakes, rivers, oceans, aquifers, and groundwater contamination. Pollution of water occurs when pollutants are discharged into water bodies directly or indirectly without adequate treatment to remove harmful compounds. The need for water quality improvement and preservation is constantly growing, being of utmost importance. But our valuable water resources are contaminated by the point and non-point sources. Due to different side effects and carcinogenic nature, this contamination is very dangerous. Here are some scary facts about the pollution of water. Two million tons of sewage, industrial and agricultural waste is released into the world's water every day, which is the equivalent of the weight of 6.8 billion people for the entire human population. According to the survey conducted by Food and Water Watch, around 3.5 billion people will be facing water shortage problems in 2025. This is mainly due to the pollution of the water. Approximately 894 million people worldwide do not have access to improved water sources, according to the World Health Organization (WHO) and United Nations Children's Fund. According to recent WHO figures, 50,000 people die every day from complications of polluted water [1]. In the textile, paper, rubber, plastics, leather, cosmetics, pharmaceutical, and food industries, methylene blue (MB) is a common dye. Discharged effluents from these industries contain residues of coloring. Therefore, the presence of very low levels of effluent is highly visible [2,3]. Discharge of colored wastewater without proper treatment can lead to numerous problems such as the water body's demand for chemical oxygen (COD) and increased toxicity. Effluents from textile plants contain portions of coloring used in industries such as textiles, paper, plastics, tannery, and paints. It is estimated that the quantity of dyes produced annually exceeds 700,000 tons, with 10%–15% discharged into wastewater, which are important sources of water pollution, can be carcinogens and toxic in some colors and their degradation products [4]. Before disposal, the dyes must be treated and their products are harmful to flora and fauna, and some are even mutagenic or cancerous [5]. Several azo dyes cause damage of deoxyribonucleic acid that can lead to the genesis of malignant tumors. Electron-donating substituents in ortho and para position can increase the carcinogenic potential. The toxicity diminished essentially with the protonation of aminic groups. In wastewater treatment, many methods have been used, such as biodegradation, ultra-filtration, photocatalytic degradation, oxidation, and adsorption [6–9]. Adsorption is a conventional wastewater treatment technique that is comparatively cheap and efficient. The efficacy of any adsorption process usually depends to a large extent on the physicochemical properties of the adsorbent used. Therefore, it is very important and meaningful to search for new adsorbents with large specific surface area, high adsorption capacity, fast adsorption rate, and special surface reactivity. There are many reports of some dyes being adsorbed on various adsorbents such as fly ash, sand, rejected tea, polymers, but no such study on graphene oxide (GO) is available. Experimental results have shown that GO is a promising adsorbent in industries such as (MB, methylene green, arsenazo III, orange G, etc.) to remove a variety of dyes. GO is an excellent adsorbent for removing from different matrixes a wide variety of contaminants. Its benefits are derived primarily from the large surface area, well-developed porous structure, and the presence of functional surface groups. GO, however, is expensive, limiting its application on a large scale. A potential cost reduction method is the production of GO from low-cost materials such as agricultural by-products. The advantage of using agricultural by-products for activated carbon production as raw materials is that they are renewable and potentially less expensive to manufacture. GO production from date pits serves the environment from two perspectives. First, it converts unwanted, surplus agricultural waste into valuable adsorbents (millions of tons are produced each year) [10]. Activated carbon is widely used as an adsorbent material in both water purification and for water treatment plants. Active carbon is characterized as a carbonaceous material with a highly porous internal structure generally derived from pyrolysis and chemical treatment of sources including wood, coal, nutshells, and other organic materials [11]. The activation process usually carried out by chemical or steam treatment at elevated temperatures, generates a large porous network within the carbonaceous material [12]. Adsorption is one of the most efficient wastewater treatment processes left after conventional effluent treatment to reduce trace hazardous organic and inorganic compounds. It is also used to remove contaminated groundwater from organic and inorganic compounds that are toxic. In water treatment, adsorption using active carbon is the most widely used method. Some reports on wastewater treatment using microwave-assisted approaches have been available in recent years. For example, in the treatment of phenolic wastewater, wet air oxidation on activated carbon under microwave irradiation was used; the application of microwave technology has become increasingly important in the treatment of pollutants in the environment. The hypothesis of this study found that if GO converted from Saudi date pits is applied to MB dye and arsenazo III dye, then the results of the degradation will be effective. This is due to the efficacy of the adsorption process and the GO's physicochemical properties and microwave technology application. Active carbon is one of the most widely used adsorbents produced from a wide range of raw materials rich in carbon, including wood, coal, peat, coconut shells, nut shells, bones, and fruit stones. The aim of this work is to determine the effectiveness of degradation of a novel technique of microwave radiation against MB dye

and arsenazo III dye using GO synthesized from Saudi date pits. Hopefully, this research will lead to the valuable real-world use of the method implemented in water filters and water treatment plants for water purification from organic pollutants.

2. Methods and measurements

2.1. Conversion of date pits to active carbon

Ten grams of date pit samples were washed with distilled water and then dried for 24 h at 105°C. Grinding and sieving to 250 μm were performed after cooling. Physical activation for date pit samples was performed by carbonizing for 2 h under N_2 gas at temperatures of 500°C, 700°C, and 900°C. Activation of samples under CO_2 gas for 2 h at 600°C, 900°C, and 1,200°C temperatures and 7.2 g with a yield of 72%.

2.2. Conversion of active carbon to GO

GO was prepared using Hammer's method [13–15]. Hummer's method is a chemical process that can be used by adding potassium permanganate to a graphite, sodium nitrate, and sulfuric acid solution to generate graphite oxide. In the creation of a single molecule thick version of the substance known as GO it can also be revised. We took 5 g of active carbon from date pits, 2.5 g of sodium nitrate, 115 ml of sulfuric acid. We add all the above materials to a beaker of 800 ml and then put the beaker in the ice bath and mix it for 20–30 min. Then, remove the beaker from the cold ice bath and place it at room temperature on the magnetic stirrer. Then added 15 g of potassium permanganate very slowly, then moving the beaker into the ultrasonic bath tub and stirring the solution for 2 h at 40°C. It was obtained dense paste. Add 500 ml of water as a solution has sulfuric acid, then add water slowly and stir it for an hour. We then added 10 ml of hydrogen peroxide with 30% concentration and stirring for another 2 h. Note, that washing (centrifuge + ultrasonic) has removed the color of your solution, inorganic anions, and impurities. You will get a 3.9 g GO powder with a yield of 78% after drying at 85°C for 24 h on a hot plate.

2.3. Microwave experiments

For the supply of microwave energy, a modified domestic microwave (MS) furnace with variable power was used. On its top cover, one hole was drilled to allow glass condensation system to be installed. Installed in MS furnace, a 500 mL Pyrex with one-necked flask reactor was connected to a water cooling condensation system (i.e., three condensers attached in one line) to allow fast and fast water vapor condensation. Fig. 1. shows a schematic illustration of the microwave experimental arrangement device.

2.4. Degradation of MB and Arsenazo III dyes

Two hundred and fifty milliliters of MB of 2.5×10^{-6} M molar was mixed and shaked with 0.1 g GO for 10 min before being transferred to the microwave system. A 250 ml
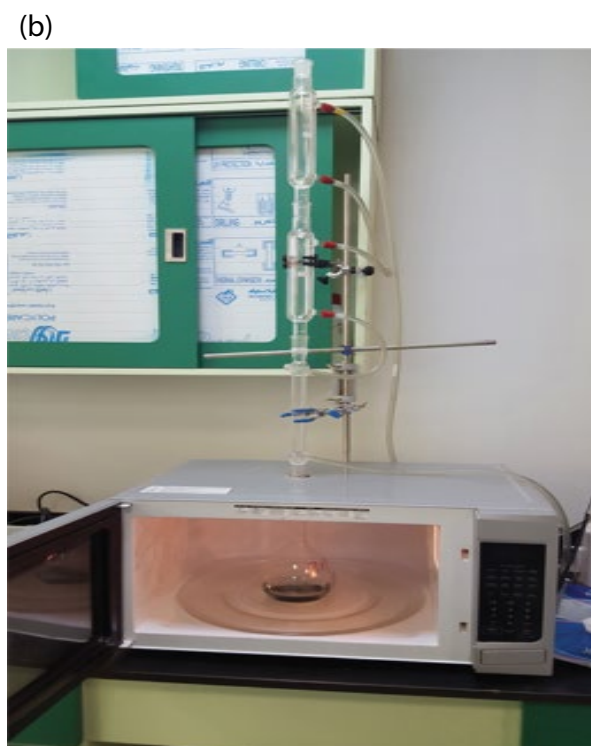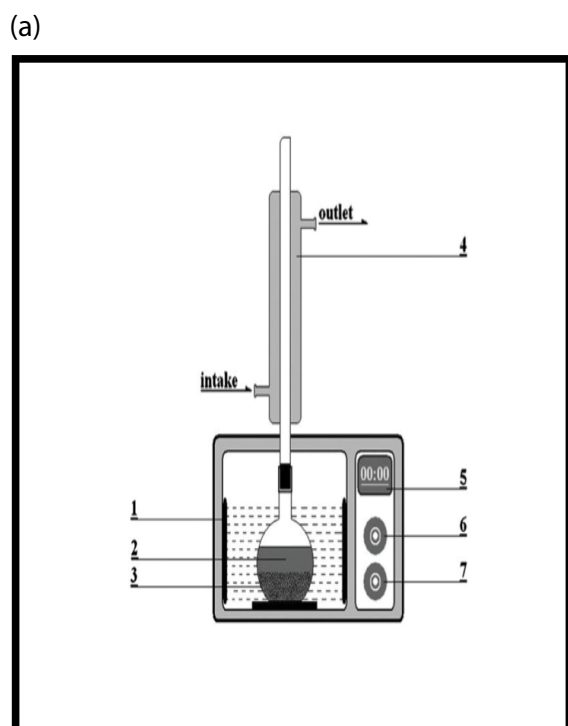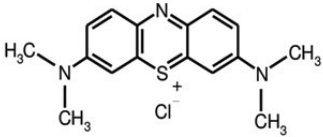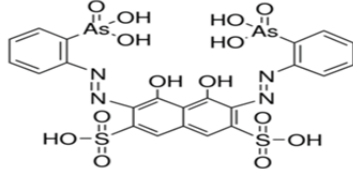

Fig. 1. (a) Schematic illustration of experimental apparatus (1) microwave generator, (2) reaction solution, (3) GO powder, (4) condenser, (5) time display, (6) time adjuster, and (7) power adjuster and (b) picture of the process of degrade the dye inside the microwave system.

of 2.510^{-6} M arsenazo III dye mixed with 0.1 g GO and shaking 10 min before being transferred to the microwave system. Table 1 shows the molecular structure of the investigated Dyes. We then applied the various parameters to select the optimum conditions for MB dye and arsenazo III dye degradation such as, time, watt and dye concentration. Fig. 2 shows a picture of the process of degrading the dye within the microwave system.

2.5. Characterization

The analysis of GO and active carbon was carried out using several methods such as scanning electron microscopy (SEM), Fourier transform (FT)/Raman, surface area, Fourier transformation infrared spectroscopy (FT-IR), and X-ray diffraction (XRD) measurement. ultraviolet-visible absorbance, JASCO (570 Japan) double beam spectrophotometer,

Table 1
The molecular structure of the investigated dyes

Dye	Chemical structure	Chemical formula	λ_{max}
MB		$C_{16}H_{18}ClN_3S$	660 nm
Arsenazo III		$C_{22}H_{18}As_2N_4O_{14}S_2$	513 nm

(a)
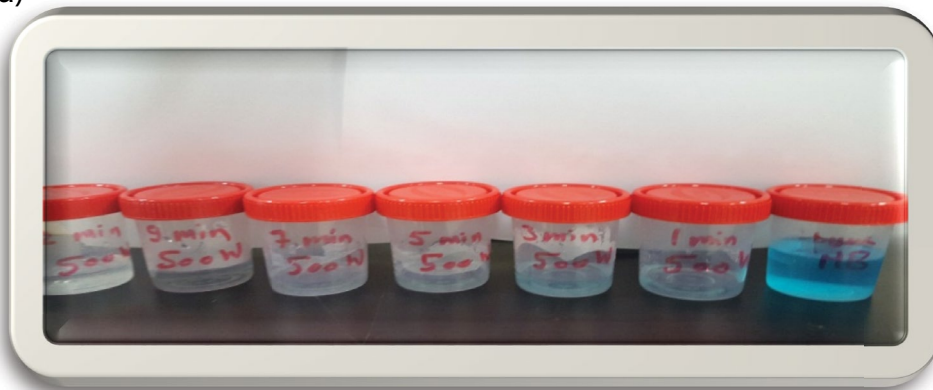
(b)

Figs. 2a and b. Picture of MB and arsenazo III dye after degradation at various times.

measured and analyzed the samples. MB and arsenazo III color degradation were monitored as a function of irradiation time by measuring maximum absorbance. Measurements were recorded for chemical oxygen demand (COD) and biological oxygen demand (BOD).

3. Results and discussions

3.1. SEM micrograph analysis

The conversion of date pits to active carbon and the conversion of active carbon to GO were analyzed with different magnification using SEM micrograph. Figs. 3a and b show the GO (H_2SO_4) SEM image analysis and the active carbon SEM image, respectively. Fig. 3a shows the fluffy morphology, and the high-resolution image shows exfoliated graphene sheets. An SEM analyzed the sample of conversion date pits to active carbon, (Fig. 3b). The physical surface morphology of converting date pits to active carbon shows that well-developed pores of a wide variety are present along with smooth surface fibrous structure. It can be seen that a possible material for removal pb^{2+} of >90% from an aqueous solution of Pb^{2+} within 40 min by the sodium dodecyl sulfate acrylamide Zr(IV) selenite (SDS-AZS) nanocomposite cation exchange material as they possessed irregular pebble-like structure with sharp edges [16].

Due to depolymerization and subsequent release of volatile organic substances from carbonization, different pore sizes, and shapes were observed on the conversion to an active carbon surface sample. Functional groups are very important features of converting date pits to an active carbon sample as they determine the carbon surface properties and their quality.

3.2. FT/Raman measurements of GO (H_2SO_4) and active carbon

In the scattering region of 400–3,200 cm^{-1}, Fig. 4 shows the GO FT/Raman (H_2SO_4) and the GO Raman (H_2SO_4) and active carbon samples have two peaks. These peaks located around 1,336 and 1,566 cm^{-1} assigned to the G resulting from the first-order. The dispersion over E2g orbitals phonon of
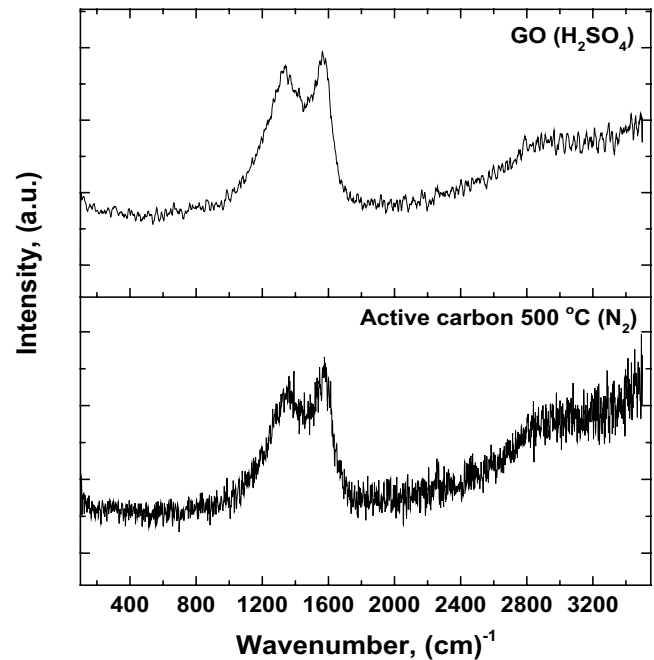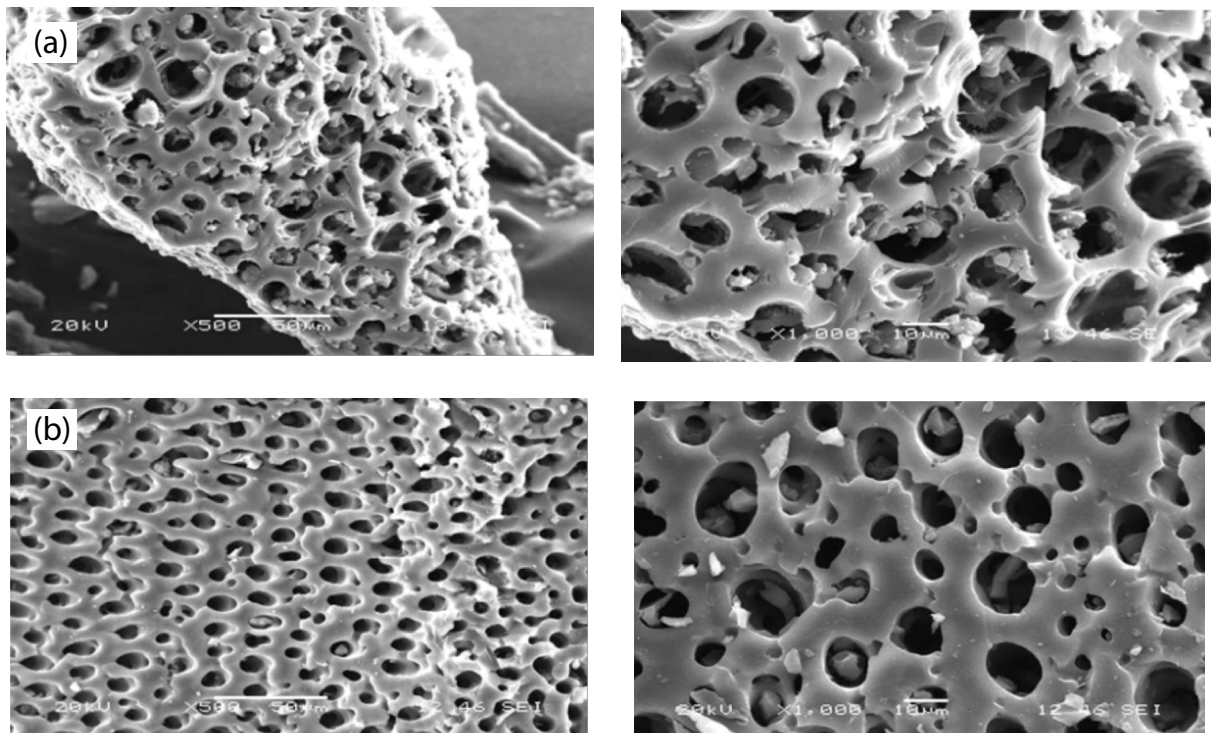

Fig. 4. FT/Raman of GO (H_2SO_4) and active carbon.

Fig. 3. SEM of GO (H_2SO_4) and active carbon. (a) SEM of Active carbon and (b) SEM of active carbon after converted to GO (H_2SO_4).

Sp2 C atoms, an indication of graphic carbon and D graphite bands resulting from a breathing mode of A1 g symmetry k-point photons reflecting the presence of disorders and the edges and boundaries of amorphous carbon domains. D-band appearance is attributed to the existence of defects due to extensive oxidation that reflects the extent of GO atomic disorder. This can also be attributed to the defects produced during pyrolysis by the decomposition of groups containing oxygen. Several investigations reported equivalent results [17,18].

3.3. Surface area measurements of GO (H_2SO_4) and active carbon

Fig. 7 displays GO (H_2SO_4) and active carbon surface measurement. For the GO (H_2SO_4) powder sample of an estimated surface area of 754 m^2/g, a relatively high GO (H_2SO_4) surface area. Meanwhile, the smallest surface area of 243 m^2/g also shows good adsorption capacity was the active carbon prepared from date pits sample. Visualize the surface area change in more detail with changes in the independent variables. It was also possible to further understand the relationship between dependent and independent variables and to achieve optimization.

3.4. FT-IR of GO (H_2SO_4) and active carbon

FT-IR analysis was done to determine the surface functional groups of GO (H_2SO_4) and active carbon as shown in Fig. 5. The wide band at 3,451 cm^{-1} shows the vibrations of hydroxyl groups. This is because of the presence of molecules of water. C=C aromatic ring stretching vibration can be assigned to the observed peak at 1,620 cm^{-1}. The 1,053 and 671 cm^{-1} peaks reveal C–O and C–H stretching vibrations.
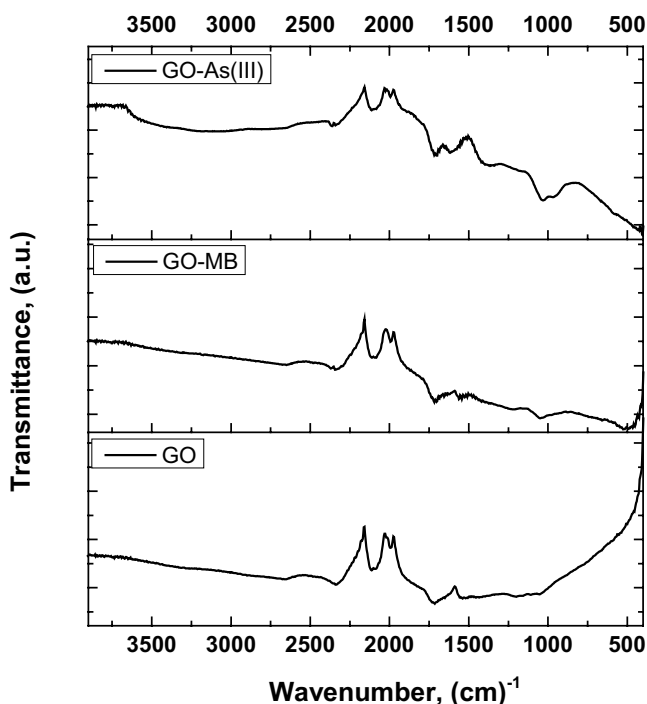
The presence of multiple oxygen functionalities reveals the GO's complex non-stoichiometric property [19]. The region between 1,610 and 1,500 cm^{-1} is associated with C–C stretching in lignin structure aromatic rings. Researchers [20,21] observe similar results for both GO and active carbon. The wide and flat band at 3,300–3,400 cm^{-1} shows the presence of alcohol, phenol, or carboxylic acid stretching vibration –OH. However, in case of adsorption of AS(III) dyes, presence of distinguish functional groups stretching vibration band of azo group (–N=N–) from 1,504 to 1,555 cm^{-1}. On the other hand, intense band with the peak at 1,593 cm^{-1} corresponds to the C=N and C=C vibrations of MB as shown in Fig. 5.

3.5. XRD measurements of GO (H_2SO_4) and active carbon

The GO (H_2SO_4) and active carbon XRD patterns are shown in Fig. 6. In the GO (H_2SO_4) and active carbon (500°C, N_2 gas) samples, the wide diffraction peak may be attributed to amorphous carbon structures. Due to the graphite structure axis [22–24], the small and week diffraction peak (2 = 40–45°). There is no noticeable difference between GO (H_2SO_4) and active carbon in the XRD diffraction patterns, suggesting that the chemical reduction process does not affect the carbon material microstructure. The XRD diffraction patterns confirmed by the SEM micrograph and the FT-IR spectra are identified as aggregating the particles due to the oxidation reaction and the presence of different functional oxygen groups.

3.6. Degradation of MB dye

Contact time is one of the most important parameters for evaluating the adsorption process's practical application. Fig. 7 shows the degradation of methylene blue dye at different times. Figs. 7–9a and b show the effect of contact time, watt and concentration on removing MB dyes in each case. The adsorption capacity of the adsorbent material (GO) with microwave radiation was investigated by removing 2.5 capacities of MB dye from aqueous solutions below 500 W and the order of efficiency was obtained. It was found from the represented Figs. 7–9a and b that GO samples showed good efficiencies in removing MB dye
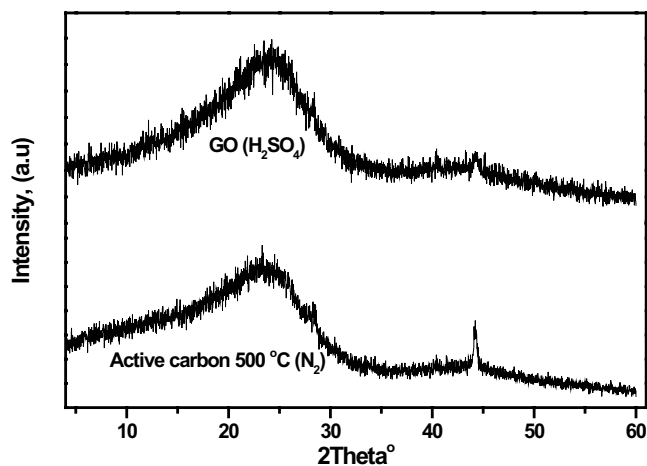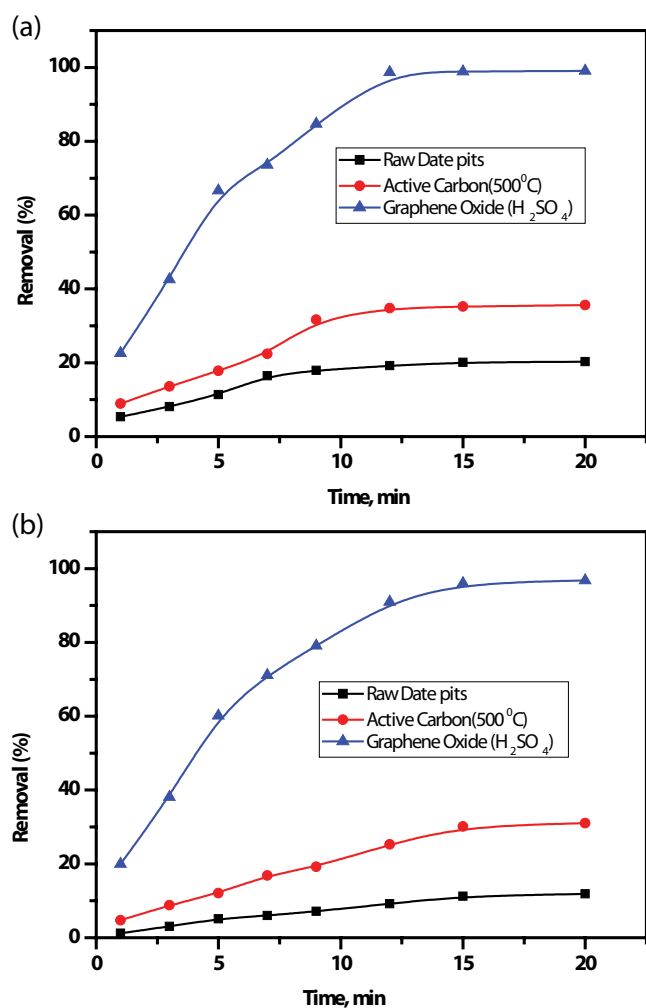
Fig. 5. FT-IR of GO, GO-MB, and GO-AS (III).

Fig. 6. XRD of GO (H_2SO_4) and active carbon.

Fig. 7. Percentage removal of (a) MB-dye vs. time at 500 W and (b) AS (III)-dye vs. time at 500 W.

Fig. 8. Effect of microwave power on % Removal of (a) MB dye and (b) arsenazo III dye through 12 min.

within 12 min with high surface areas. GO and active carbon rates were 98.7% and 34.8%, respectively. In removing MB dye within 15 min the adsorption capacity of the adsorbent material (GO) without using microwave radiation was investigated at a rate of 12.74% (adsorption processes). Also activated carbon synthesized from peanut was sufficiently efficient in removal if heavy metals like Cr^{6+} [25]. Methods for determining organic matter in wastewater are widely used for monitoring COD and BOD. The pre- and post-degradation of MB dye is shown in Table 2 using COD and BOD measurements. The COD was found before dye removal was 450 mg/L, while 87 mg/L was found after dye removal, and 270 mg/L was found before dye removal, and reaches to 12 mg/L was found after dye removal.

3.7. Degradation of arsenazo III dye

The adsorption capacity of the adsorbent material (GO) with microwave radiation was investigated in the removal of 2.5×10^{-6} M of arsenazo III dye from aqueous solutions under 500 W, and the order of efficiency was obtained while nickel ferrite bearing nitrogen-doped mesoporous carbon
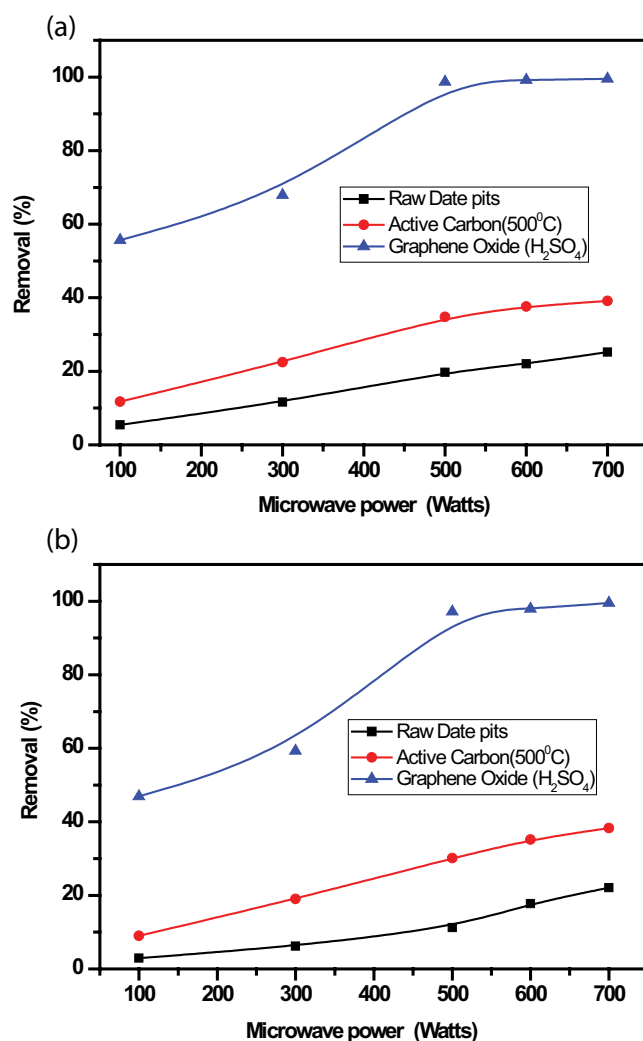
$(NiFe_2O_4\text{-NC})$ was produced from aqueous media using polymer bimetal complexes and used for Hg^{2+} removal [26]. Fig. 7 shows the degradation of arsenazo III dye at different times. From the represented data, it was found GO samples, with high surface area, showed good efficiencies in the removal of arsenazo III dye within 15 min. The rates of GO and active carbon were, respectively, 96.06% and 30.13%. In the removal of arsenazo III within 15 min the adsorption capacity of the adsorbent material (GO) without the use of microwave radiation was investigated. The COD before dye removal was 580 and 118.6 mg/L after dye removal and 310 mg/L before dye removal and 21.75 mg/L after dye removal.

3.8. Mechanism of degradation

Briefly, the reactants need to be activated for a chemical reaction to occur. Heating is a conventional method of activating a reactive medium in chemistry. Temperature elevation induces an increase in kinetic energy in molecules and
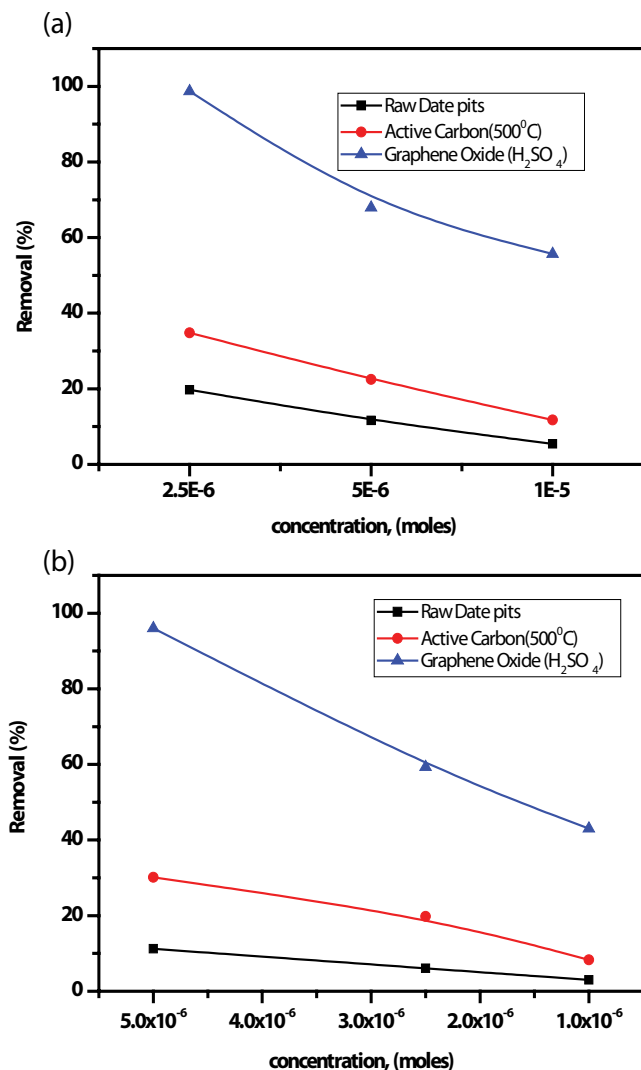
(a)

(b)

Fig. 9. Percentage removal of (a) MB dye vs. the concentrations at 500 W for 12 min and (b) AS (III) dye vs. the concentrations at 500 W for 12 min.

Table 2a
COD and BOD measurements for degradation of MB dye by using GO

	Before	After	Rate%
COD	450 mg/L	87 mg/L	80.6%
BOD	270 mg/L	12.8 mg/L	95.2%

Table 2b
COD and BOD measurements for degradation of arsenazo III Dye by using GO

	Before	After	Rate%
COD	580 mg/L	118.6 mg/L	79.5%
BOD	310 mg/L	21.75 mg/L	93%

therefore increases the rate of collision. However, only a few have sufficient energy and proper orientation to lead to the product among these collisions. Heating causes molecules to be isotropically excited, which is why all collisions are ineffective. An excitation tool that could favor efficient collisions by modifying the energy distribution of molecules could increase the reaction rate, according to the Eyring formulation. GO, a strong microwave absorbent, can substantially absorb and transfer MW energy under MW irradiation, indicating that a strong absorbent could generate large amounts of "hot spots," which could increase molecular degradation [27,28]. The electrophilic oxygen ions (O_2-, $O-$, and O_2-) derived from GO lattice oxygen show high activity in catalytic reactions and may be involved in MB or AS(III) degradation [29]. Lattice oxygen vacancies have recently been replenished by dissolved molecular oxygen in solution, known as the mechanism of Mars van Krevelen [30]. Since the energy of microwave photons is too low (about 10–5 ev) compared to chemical bonds, the absorption of microwave photons can induce no breakdown of chemical bonds. MW cannot therefore induce any shift in chemical equilibrium but can accelerate the degraded rate of MB. This means that microwave and GO combined simultaneously can effectively degrade MB and AS(III) to total carbon dioxide and water. Metal organic frame works (MOFs) showed outstanding results. So, we expect intense study attempts to focus on MOFs and their composites, with emphasis on their practical use in sewage therapy [31]. The ordered porous structure and the high GO surface area create more catalytic sites to provide extra pathways for electrons migration and enable better contact between reactants and active sites and led to the separation of charge carriers. Different interactions could easily sorb the MB and AS(III) molecules to the GO surface. Like nanocomposite starch/SnO_2 material was used as an adsorbent for removing from the aqueous medium the highly toxic Hg^{2+} metal ions [32]. Such adsorption significantly increases the effective concentration of molecules of MB and AS(III) close to the GO surfaces Microwaves can promote the release of hydroxyl radicals from GO, thus improving the system's oxidative capacity. Due to the loss of graphene at microwave frequencies, its absorption will strongly affect the patch's radiation properties and enhance the degradation MB and AS(III).

GO is one of the most promising Graphene derivatives. It is a hybridized, two-dimensional (2D) sp2 single carbon atom with epoxide, hydroxyl, carboxylic, and carbonyl groups that contain oxygen. It was used to improve the mechanical, chemical, thermal, and electrical properties of composite materials in various applications as an economical carbon precursor [33,34]. While GO has had remarkable adsorption results in azo dyes decontamination, GO as a practical adsorbent in the treatment of wastewater is restricted by the high colloidal resistance of 2D GO and its tendency to aggregate through strong π-π interaction [35]. Graphene adsorption data was briefly screened by Khurana et al. [36]. Electrostatic interaction is one of the core adsorption mechanisms. There are a number of groups containing oxygen on GO, which are negatively charged, according to the GO structure. Positive contaminants such as heavy metal ions, cationic dyes and other positive contaminants prefer a negative GO. Once deprotonation of carboxylic groups is

put into the basic environment will be enhanced [37–39]; higher performance is therefore to be demonstrated by GO. The use of reduced graphene oxide (rGO) was shown to effectively remove Malachite green (MG) [40] from simulated wastewater. The possible ways in which MG dye can interact with rGO are derived from rGO's nanostructural characteristics. The combination of the interactions between the aromatic MG ring and graphitic structure, and the interaction between the cationic MG dye core and the π-electron clouds and the negative residual rGO oxygen features promotes MG's collectively adsorption on the rGO. The adsorption capacity of rGO for MG is 0.476 g/g. The ability to adsorb varies with experimental conditions, design and nature of adsorbent. The adsorption of dyes on few-layered graphene nanosheets is possible using the strength of Van der Waals and π–π stacking to change the physical and chemical properties to improve the manufacture of reduced graphene. The layers of rGO and of single GO have high aspect ratios and large and π- electronic surfaces that give strong inter-molecular forces among adsorbates [41]. rGO was already used to remove cationic MB as adsorbents [42–44]. rGO was also used by Guo et al. [45] to adsorb reactive red (RR) dye. The Langmuir model showed a total adsorption capacity of 0.03216 g/g. Furthermore, experimental kinetic data were analyzed in the first-order and second-order models of the equation. The pseudo-second model proved the best model for the adsorption process, which implies that the adsorption could be regulated through a sharing of electrons or covalent forces through the chemical rate-limiting stage. Another dye, also with graphene composite adsorbent, was studied. Nuengmatcha et al. [46] investigated GO in comparison with bare graphite powder (BGP), for the adsorption of Alizarin Red S (ARS) with GO as an adsorbent. The GO adsorbed capacity was 0.8850 g/g, higher than BGP (0.3413 g/g) adsorbed. The kinetic adsorption is well fitted with the pseudo kinetics of the second order. The model of intra-particle diffusion defined the diffusion of the intra-particle not as the only rate limit. The bio-composite product of the adsorption process was synthesized by Bhattacharyya et al. [47] includes GO, cross-linker glutaraldehyde and potato starch (GO-GLu-starch) was applied for adsorption of MB dye with adsorption capacity of 0.256 g/g. The kinetics of the pseudo-second-order reveals that the surface bond of adsorbents and adsorbed molecules has occurred. The Freundlich isotherm shows that the major part of the adsorption takes place through the electrostatic attraction between an adsorbent and adsorbate molecules.

3.9. Adsorption kinetics

The amount adsorbed of dye onto the GO studied with time for estimating the adsorption mechanism. The adsorption of two dyes with time shows that mixing period of 15 min is optimum for attaining the equilibrium, these findings reflect a fast kinetic for adsorption of MB onto the prepared GO.

Different kinetic models were applied on the obtained results and the kinetic parameters were determined. The kinetic models correlate the amount adsorbed of dye with time. Lagergren equation describe and used to the kinetic data in the adsorption systems. In addition, this Eq. (1)

developed by assuming both diffusional and surface reaction kinetic models for pseudo-first-order reactions [48].

$$\frac{dq_t}{dt} = k_1(q_e - q_t) \tag{1}$$

where q_e and q_t are the dye concentration in solid phase at equilibrium and at time t, respectively, and k_1 is the model constant (min^{-1}). The linear form of the above equation was obtained by integration at the borders ($q_t = 0$ to $q_t = q_t$ and $t = 0$ to $t = t$) as:

$$\log(q_e - q_t) = \log q_e - \frac{k_1 t}{2.303} \tag{2}$$

The rate constant, k_1 was determined from the plot of $\log(q_e - q_t)$ with t while the value of q_e was determined from the intercept. The model variables with the coefficient are given in Table 3.

The plots in the figures above show linear fit with correlation coefficient of 0.798 for MB, 0.889 with AS(III), respectively. The values of calculated adsorption capacity q_e and the linear regression coefficient clarify that the studied kinetic model could not fit with the experimental results for adsorption of MB and AS(III) onto GO.

Second order kinetic model, which describe the chemical adsorption is given by the following Eq. (3) [49].

$$\frac{dqt}{dt} = k_2(q_e - q_t)^2 \tag{3}$$

where k_2 is the model constant (g/mg min). Eq. (3) could be integrated at the border ($q_t = 0$ to $q_t = q_t$ at $t = 0$ to $t = t$) to be:

$$\frac{t}{q_t} = \frac{1}{k_2 q_e^2} + \frac{t}{q_e} \tag{4}$$

The model variables were calculated from the plot of t/q_t with t. The plot showed a linear relation, and the model parameters with the previous work are given in Table 3.

The results of the studied kinetic model clarify that the experimental results for adsorption of MB and AS(III) onto GO could be described by kinetic model supporting chemical adsorption. The sorption of MB and AS(III) could be favorably described by the pseudo-second-order kinetic model. This finding refers to the participation of chemical adsorption within the adsorption mechanism for MB and AS(III) onto GO.

Elovich kinetic model was applied upon the results to explain mainly the chemisorptions onto heterogeneous solid surfaces. The linearized form of Elovich model Eq. (5) is [50]:

$$q_t = \left(\frac{1}{\beta}\right)\ln(\alpha\beta) + \left(\frac{1}{\beta}\right)\log t \tag{5}$$

where α and β are model parameters representing the starting sorption rate (g mg^{-1} min^{-2}) and the leaching constant (mg g^{-1} min^{-1}), correspondingly. The model parameters were

Table 3
Comparative study of adsorption parameters with previous kinetic data

Adsorption system	Kinetic model	Parameters	References
MB-GO	Pseudo-first-order	$k_1 = 1.718$ $q_e = 0.607$	Present work
	Pseudo-second-order	$K_2 = 2.18$ $q_e = 2.73$	Present work
	Elovich	$\beta = 5.98$ $\alpha = 8.72$	Present work
AS(III)-GO	Pseudo-first-order	$k_1 = 2.692$ $q_e = 0.635$	Present work
	Pseudo-second-order	$K_2 = 26.8$ $q_e = 2.121$	Present work
	Elovich	$\beta = 3.46$ $\alpha = 7.21$	Present work
MG-rGO	Pseudo-first-order	$q_e = 0.467$	[41]
MB-GO	Pseudo-first-order	$q_e = 0.714$	[43]
RR-rGO	Pseudo-second-order	$q_e = 0.032$	[45]
ARS-GO	Pseudo-second-order	$q_e = 0.089$	[46]
MB-GO (glu-Starch)	Pseudo-second-order	$q_e = 0.256$	[47]

calculated from the linear fit of q_t vs. $\log(t)$ plot, and the data presented in Table 3.

The value Elovich constant α and β adsorption of MB AS(III) onto GO refereeing to the effect of adsorbent dose and the possibility of performing sorption-desorption regeneration cycles of adsorbent. The value of correlation coefficient (R) reflect a poor fit of Elovich model with the experimental results.

It could be inferred that both chemical and surface adsorption mechanisms are participating in the studied systems.

Adsorption occurs frequently with the reverse desorption process, which demonstrates the transfer of sorbate ions from the surface to the solution. Sorbent regeneration can be measured better depending on the amount of orbit desorbed from the adsorbent, changes in desorption, and also increases in the sorbent's renewal process (Mishra [51]; Peng et al. [52]). There may be physical or chemical adsorption. This depends on the type of adsorbent-adsorbent interaction. The increase in sorbate quantity at the interface is due to non-specific van der Waals forces in the case of physical adsorption. Chemical adsorption (chemisorptions) is caused by chemical reactions between the adsorbent and the sorbate which create ionic or covalent bonds. The former is weakly reversible, general, its thermal effect is low (kJ/mol units), while its energy varies from tens to hundreds of kJ/mol (Virendra Singh et al. [53]; Tripathi and Ranjan [54]).

4. Conclusion

This research proved the hypothesis by effectively demonstrating viable results using Saudi date pits as a raw material for GO preparation to remove MB and arsenazo III dye from wastewater. GO derived from date pits is now promised to be used as a potential adsorbent for high-capacity organic dyes. The treated GO will be adopted as a catalyst in this regard and the microwave will be used as a source of irradiation. Using warm water (45°C) for 20 min, the GO could be reused. Organic pollutants can be quickly and completely degraded in a short time frame. His new technology for wastewater treatment reveals many benefits, such as full and rapid degradation, low cost, no intermediate products, and no secondary pollution.

References

[1] Y. Liu, S. Yang, J. Hong, C. Sun, Low-temperature preparation and microwave photocatalytic activity study of TiO_2-mounted activated carbon, J. Hazard. Mater., 142 (2007) 208–215.

[2] M. Alkan, O. Demirbas, Celikc, S. Apa, M. Dogan, Sorption of acid red 57 from aqueous solutions onto sepiolite, J. Hazard. Mater., 116 (2004) 135–145.

[3] K. Turhan, S.A.Ozturkcan, Decolorization and degradation of reactive dye in aqueous solution by ozonation in a semi-batch bubble column reactor, Water Air Soil Pollut., 224 (2012) 1353–1357.

[4] H.I. Owamah, I.S. Chukwujindu, A.K. Asiagwu, Biosorptive capacity of yam peels waste for the removal of dye from aqueous solutions, Civ. Environ. Res., 3 (2013) 36–48.

[5] L. Fan, C. Luo, M. Sun, X. Li, F. Lu, H. Qiu, Preparation of novel magnetic chi-tosan/graphene oxide composite as effective adsorbents toward methylene blue, Bioresour. Technol., 114 (2012) 703–706.

[6] A. Walcarius, L. Mercier, Mesoporous organosilica adsorbents: nanoengineered materials for removal of organic and inorganic pollutants, J. Mater. Chem., 20 (2010) 4478–4511.

[7] B.V. Bruggen, C. Vandecasteele, Removal of pollutants from surface water and groundwater by nanofiltration: overview of

possible applications in the drinking water industry, Environ. Pollut., 122 (2003) 435–445.

[8] L.K. Posey, M.G. Viegas, A.J. Boucher, C. Wang, K.R. Stambaugh, M.M. Smith, B.G. Carpenter, B.L. Bridges, S.E. Baker, D.A. Perry, Surface-enhanced vibrational and TPD study of Nitroaniline isomers, J. Phys. Chem. C, 111 (2007) 12352–12360.

[9] C.M. Chen, A.C. Lua, Lung toxicity of paraquat in the rat, J. Toxicol. Environ. Health Part A, 60 (2000) 477–487.

[10] N.S. Awwad, A.A. El-zahhar, A.M. Fouda, H.A. Ibrahium, Removal of heavy metal ions from ground and surface water samples using carbons derived from date pits, J. Environ. Chem. Eng., 1 (2013) 416–423.

[11] N. Ando, Y. Matsui, R. Kurotobi,; Y. Nakano, T. Matsushita, K. Ohno, Comparison of natural organic matter adsorption capacities of super-powdered activated carbon and powdered activated carbon, Water Res., 44 (2010) 4127–4136.

[12] M.A. Yahya, Z. Al-Qodah, C.W.Z. Ngah, Agricultural bio-waste materials as potential sustainable precursors used for activated carbon production: a review, Renewable Sustainable Energy Rev., 46 (2015) 218–235.

[13] P.G. Ren, D.X. Yan, X. Ji, T. Chen, Z.M. Li, Temperature dependence of graphene oxide reduced by hydrazine hydrate, Nanotechnology, 22 (2011) 055705–055713.

[14] W. Hummer, R. Offeman, Preparation of graphite oxide, J. Am. Chem. Soc., 80 (1958) 1339–1339.

[15] N.N. Zhang, H.X. Qiu, Y. Liu, W. Wang, Y. Li, X.D. Wang, J.P. Gao, Fabrication of gold nanoparticle/graphene oxide nanocomposites and their excellent catalytic performance, J. Mater. Chem., 21 (2011) 11080–11083.

[16] M. Naushad, Surfactant assisted nano-composite cation exchanger: development, characterization and applications for the removal of toxic Pb^{2+} from aqueous medium, Chem. Eng. J., 235 (2014) 100–108.

[17] Z.J. Fan, W. Kai, J. Yan, T. Wei, L.J. Zhi, J. Feng, Y.M. Ren, L.P. Song, F. Wei, Facile synthesis of graphene nanosheets via Fe reduction of exfoliated graphite oxide, ACS Nano, 5 (2011) 191–198.

[18] H. Li, G. Zhu, Z.H. Liu, Z. Yang, Z. Wang, Fabrication of a hybrid graphene/layered double hydroxide material, Carbon, 48 (2010) 4391–4396.

[19] M. Veerapandian, M.H. Lee, K. Krishnamoorthy, K. Yun, Synthesis, characterization and electrochemical properties of functionalized graphene oxide, Carbon, 50 (2012) 4228–4238.

[20] C. Pasquali, H. Herrera, Pyrolysis of lignin and IR analysis of residues, Thermochim. Acta, 293 (1997) 39–46.

[21] I. Ozdemir, M. Şahin, R. Orhan, M. Erdem, Preparation and characterization of activated carbon from grape stalk by zinc chloride activation, Fuel Process. Technol., 125 (2014) 200–206.

[22] M. Hara, T. Yoshida, A. Takagaki, T. Takata, J.N. Kondo, S. Hayashi, K. Domen, A carbon material as a strong protonic acid, Angew. Chem. Int. Ed., 43 (2004) 2955–2958.

[23] M. Toda, A. Takagaki, M. Okamura, J.N. Kondo, S. Hayashi, K. Domen, M. Hara, Biodiesel made with sugar catalyst, Nature, 438 (2005) 178–178.

[24] S. Suganuma, K. Nakajima, M. Kitano, D. Yamaguchi, H. Kato, S. Hayashi, M. Hara, Hydrolysis of cellulose by amorphous carbon bearing SO_3H, COOH, and OH groups, J. Am. Chem. Soc., 130 (2008) 12787–12793.

[25] Z.A. AL-Othman, R. Ali, Mu. Naushad, Hexavalent chromium removal from aqueous medium by activated carbon prepared from peanut shell: adsorption kinetics, equilibrium and thermodynamic studies, Chem. Eng. J., 184 (2012) 238–247.

[26] M. Naushad, T. Ahamad, B.M. Al-Maswari, A.A. Alqadami, S.M. Alshehri, Nickel ferrite bearing nitrogen-doped meso-porous carbon as efficient adsorbent for the removal of highly toxic metal ion from aqueous medium, Chem Eng. J., 330 (2017) 1351–1360.

[27] L. Zhang, X. Zhou, X. Guo, X. Song, X. Liu, Investigation on the degradation of acid fuchsin induced oxidation by $MgFe_2O_4$ under microwave irradiation, J. Mol. Catal. A: Chem., 335 (2011) 31–37.

[28] C. Marún, L.D. Conde, L.S. Sui, Catalytic oligomerization of methane via microwave heating, J. Phys. Chem. A, 103 (1999) 4332–4340.

[29] W.H. Kuan, Y.C. Chan, pH-dependent mechanisms of methylene blue reacting with tunneled manganese oxide pyrolusite, J. Hazard. Mater., 239 (2012) 152–159.

[30] C. Doornkamp, V. Ponec, The universal character of the Mars and Van Krevelen mechanism, J. Mol. Catal. A: Chem., 62 (2000) 19–32.

[31] A.A. Alqadami, M. Naushad, Z.A. Alothman, A.A. Ghfar, Novel metal−organic framework (MOF) based composite material for the sequestration of U(VI) and Th(IV) metal ions from aqueous environment, ACS Appl. Mater. Interfaces, 9 (2017) 36026–36037.

[32] M. Naushad, T. Ahamad, G. Sharma, A.H. Al-Muhtaseb, A.B. Albadarin, M.M. Alam, Z.A. ALOthman, S.M. Alshehri, A.A. Ghfar, Synthesis and characterization of a new starch/SnO_2 nanocomposite for efficient adsorption of toxic Hg^{2+} metal ion, Chem. Eng. J., 300 (2016) 306–316.

[33] F.V. Ferreira, F.S. Brito, W. Franceschi, E.A.N. Simonetti, L.S. Cividanes, M. Chipara, K. Lozano, Functionalized graphene oxide as reinforcement in epoxy based nanocomposites, Surf. Interfaces, 10 (2018) 100–109.

[34] A. Hosseinzadeh, S. Bidmeshkipour, Y. Abdi, E. Arzi, S. Mohajerzadeh, Graphene based strain sensors: a comparative study on graphene and its derivatives, Appl. Surf. Sci., 448 (2018) 71–77.

[35] B.Y.Z. Hiew, L.Y. Lee, X.J. Lee, S. Thangalazhy-Gopakumar, S. Gan, S.S. Lim, G.T. Pan, T.C.K. Yang, W.S. Chiu, P.S. Khiew, Review on synthesis of 3D graphene-based configurations and their adsorption performance for hazardous water pollutants, Process Saf. Environ., 116 (2018) 262–286.

[36] I. Khurana, A. Saxena, J.M. Khurana, P.K. Rai, Removal of dyes using graphene-based composites: a review, Water Air Soil Pollut., 228 (2017) 174–180.

[37] A. Lerf, H. He, M. Forster, J. Klinowski, Structure of graphite oxide revisited, J. Phys. Chem. B, 102 (1998) 4477–4482.

[38] A. Lerf, Graphite Oxide Story: From the Beginning Till the Graphene Hype, A.M. Dimiev, S. Eigler, Eds., Graphene Oxide: Fundamentals and Applications, Wiley, USA, 2017, pp. 3–36.

[39] Y. Cui, Y.H. Lee, J.W. Yang, Impact of carboxyl groups in graphene oxide on chemoselective alcohol oxidation with ultra-low carbocatalyst loading, Sci. Rep. 7 (2017) 3146.

[40] K. Gupta, O.P. Khatri, Reduced graphene oxide as an effective adsorbent for removal of malachite green dye: plausible adsorption pathways, J. Colloid Interface Sci., 501 (2017) 11–21.

[41] P.A. Denis, F. Iribarne, A first-principles study on the interaction between alkyl radicals and graphene, Chem. Eur. J. 18 (2012) 7568–7574.

[42] S.T. Yang, S. Chen, Y. Chang, A. Cao, Y. Liu, H. Wang, Removal of methylene blue from aqueous solution by graphene oxide, J. Colloid Interface Sci., 359 (2011) 24–29.

[43] B. Li, H. Cao, G. Yin, $Mg(OH)_2$@reduced graphene oxide composite for removal of dyes from water, J. Mater. Chem., 21 (2011) 13765–13768.

[44] H. Sadegh, G.A.M. Ali, V.K. Gupta, A.S.H. Makhlouf, R.S. Ghoshekandi, M.N. Nadagouda, M. Sillanpa, M. Elżbieta, The role of nanomaterials as effective adsorbents and their applications in wastewater treatment, J. Nanostruct. Chem., 7 (2017) 1–14.

[45] X. Guo, L. Qu, M. Tian, S. Zhu, X. Zhang, X. Tang, K. Sun, Chitosan/graphene oxide composite as an effective adsorbent for reactive red dye removal, Water Environ. Res., 88 (2016) 579–588.

[46] P. Nuengmatcha, R. Mahachai, S. Chanthai, Adsorption capacity of the as-synthetic graphene oxide for the removal ofalizarin red S dye from aqueous solution, Orient. J. Chem. 32 (2016) 1399–1410.

[47] A. Bhattacharyya, B. Banerjee, S. Ghorai, D. Rana, I. Roy, G. Sarkar, N. Saha, S. De, T.K. Ghoshd, S. Sadhukhan, D. Chattopadhyay, Development of an auto-phase separable and reusable graphene oxide-potato starch based cross-linked bio-composite adsorbent for removal of methylene blue dye, Int. J. Biol. Macromol., 116 (2018) 1037–1048.

[48] S. Lagergren, About the theory of so-called adsorption of soluble substances, Kungliga Svenska Ventenskapsakademiens Handlingar, 24 (1898) 1–39.

[49] Y.S. Ho, E. McKay, The kinetics of sorption of basic dyes from aqueous solution by sphagnum moss peat, Can. J. Chem. Eng., 76 (1998) 822–827.

[50] Y.S. Ho, G. McKay, Application of kinetic models to the sorption of copper(II) onto peat, Sci. Technol., 20 (2002) 797–815.

[51] S.P. Mishra, Adsorption-desorption of heavy metal ions, Curr. Sci. India, 107 (2014), 601–612.

[52] W. Peng, H. Li, Y. Liu, Sh. Song, A review on heavy metal ions adsorption from water by graphene oxide and its composites, J. Mol. Liq., 230 (2017) 496–504.

[53] V. Singh, D. Joung, L. Zhai, S. Das, S.I. Khondaker, S. Seal, Graphene based materials, past, present and future, Prog. Mater. Sci., 56 (2011) 1178–1271.

[54] A. Tripathi, M.R. Ranjan, Heavy metal removal from wastewater using low cost adsorbents, J. Biorem. Biodegrad., 6 (2015) 315–319.